arXiv:astro-ph/9901220v1 17 Jan 1999

The Gravitational-wave contribution to the CMB Anisotropies

Alessandro Melchiorri[1]

Dipartimento di Fisica, Universitá di Roma Tor Vergata

Via della Ricerca Scientifica, 00133 Roma, Italy

and

Département de Physique Théorique, Université de Genéve

24 Quai Ernest Ansermet, Ch-1211 Genéve, Switzerland

Mikhail Vasil'evich Sazhin[3], Vladimir V. Shulga[4]

P. K. Sternberg Astronomical Institute

Universitetskii pr. 12, 119899 Moscow, Russia

Nicola Vittorio[2]

Dipartimento di Fisica, Universitá di Roma Tor Vergata

Via della Ricerca Scientifica, 00133 Roma, Italy

Received _____; accepted _____

[1] *e-mail: melchiorri@roma2.infn.it*

[2] *e-mail: vittorio@roma2.infn.it*

[3] *e-mail: sazhin@sai.msu.su*

[4] *e-mail: shulga@sai.msu.su*

ABSTRACT

We study the possible contribution of a stochastic gravitational wave background to the anisotropy of the cosmic microwave background (CMB) in cold and mixed dark matter (CDM and MDM) models. We test this contribution against recent detections of CMB anisotropy at large and intermediate angular scales. Our likelihood analysis indicates that models with blue power spectra ($n \simeq 1.2$) and a tensor to the scalar quadrupole ratio of $R = C_2^T/C_2^S \sim 2$ are most consistent with the anisotropy data considered here. We find that by including the possibility of such background in CMB data analysis it can drastically alter the conclusion on the remaining cosmological parameters.

Subject headings: cosmic microwave background, gravitational waves, dark matter

1. Introduction

Inflationary theory has had a large impact on cosmology. On the one hand, it resolves some difficulties of the standard Big-Bang model. On the other, it provides a way of producing those density fluctuations that in the gravitational instability scenario are the seed of the large scale structure of the universe. In fact, one of the most reliable predictions of the inflationary paradigm is the parallel production of scalar and tensor perturbations from quantum fluctuations of the inflaton field $\hat{\phi}$ (Starobinsky 1979; Rubakov *et.al.* 1982; Starobinsky 1982; Abbot & Wise 1984). The amplitude of tensor fluctuations determines the value of the inflationary potential and, together with other inflationary parameters, its first two derivatives (see *e.g.* Turner 1997). Thus, a detection of a nearly scale-invariant stochastic gravitational wave (GW) background (tensor modes) is crucial in order to confirm any inflationary model and constrain the physics occurring near the Planck scale, at $\sim 10^{16} GeV$.

Observations of Cosmic Microwave Background (CMB) anisotropy promise to be unique in this respect (Starobinsky 1985; Crittenden *et.al.* 1993; Turner *et.al.* 1993). Recent numerical simulations (Zaldarriaga *et.al.* 1997; Dodelson *et.al.* 1997; Bond 1997) have shown that inflationary parameters will be measured with an accuracy of few percent by the MAP (Bennett *et.al.* 1995) and Planck (Bersanelli *et.al.* 1996) space missions, which will image the CMB anisotropy pattern with high sensitivity and at high angular resolution.

Meanwhile, the number of experiments reporting detections of anisotropy has increased to a couple of ten (see Table 1, below). At the moment, the detections available seem compatible with the predictions of inflationary models, like Cold Dark Matter (CDM), with "blue" power spectra, i.e. $P(k) = Ak^{n_S}$ with $n_S \gtrsim 1$ (de Bernardis *et.al.* 1997; Bennett *et.al.* 1996; Bond & Jaffe 1996). As noticed by many authors, there is a substantial rise in the anisotropy angular power spectrum at $\ell \sim 200$, which appears to be consistent with the expected location of the first Doppler peak in flat models. This small scale behaviour seems to disfavor a GW contribution. In fact, as is well known, tensor fluctuations induce anisotropy only on large angular scales ($\ell \lesssim 30$). If there is a sizable contribution from GW in large scale detected anisotropies, this would lower the predicted value of $(\Delta T/T)_{rms}$ on smaller scales.

Moreover, inflationary models that predict $n_S \gtrsim 1$ generally predict vanishingly small tensor fluctuations (Kolb & Vadas 1994).

Based on these arguments, a lot of recent CMB data analysis (Lineweaver *et.al.* 1997; Hancock *et.al.* 1997) has not taken into account the possible presence of a GW background, assuming its contribution to be negligible.

In our opinion, there are two points that can alter these conclusions:

- Tensor modes are compatible with the theory of linear adiabatic perturbations of a homogeneous and isotropic universe. Like scalar perturbations and in contrast with vector perturbations, they can arise from small deviations from the isotropic Friedmann universe near the initial singularity. So, CMB data should be analyzed without any *a priori* assumptions: the presence or absence of a tensor component in models with $n_S \geq 1$ can be only tested by observation.

- Few variations in the still undetermined cosmological parameters (like the baryonic abundance or the Hubble constant) and inflationary parameters (like the spectral index n_S) can counterbalance the effect of tensor modes, increasing the predicted value of $(\Delta T/T)_{rms}$ on small scales.

Thus, in this *paper*, we will discuss what kind of constraint present CMB anisotropy data provide on the tensor contribution allowing all the remaining parameters to vary freely in their acceptable ranges. We will extend our previous CMB data analysis (de Bernardis *et.al.* 1997), by including new CMB detections, and by analyzing a larger set of models. We restrict ourselves to critical universes ($\Omega_{matter} = 1$), as a recent analysis of CMB anisotropies and galaxy surveys (Gawiser & Silk 1998) has shown that pure scalar Mixed Dark Matter (MDM) models are in good agreement with the data set. We will address the importance of a cosmological constant, reported by Riess *et.al.* 1998 and Perlmutter *et.al.* 1998, in a forthcoming paper.

Since we treat the GW contribution as a free parameter, we will not test any specific inflationary model. So, our approach will be mainly phenomenological: we assume that GW are created in the early universe by some process during or immediately after inflation, which we do not want to specify any further here. Nonetheless, as the amplitude of the GW spectrum provides a test for inflation (see next section), in our conclusions we will discuss if results are compatible with this paradigm.

Since any possible GW signal will affect the matter power spectrum normalization inferred from COBE, we will test the models that best fit the CMB data with the normalization σ_8 of the matter fluctuation in $8h^{-1}$ spheres and with the shape of the spectrum from the Peacock & Dodds 1994 analysis.

The plan of the paper is as follows. In Sect.2 we write the set of equations necessary to describe the inflationary process in the slow roll approximation. In Sect.3 we briefly discuss the analysis of the current degree-scale CMB experiments. In Sect.4 we test the best fit models with the Large-Scale Structure (LSS) data. Finally, in Sect. 5 we present and discuss our conclusions.

2. Early Universe

Inflation in the early universe is determined by the potential $V(\hat{\phi})$, where $\hat{\phi}$ can be a multiplet of scalar fields. Here we restrict ourselves to the case of a single, minimally coupled scalar field ϕ with potential V and equation of motion

$$\ddot{\phi} + 3H\dot{\phi} + V' = 0, \tag{1}$$

(as usual, the dot and prime indicate derivatives with respect to physical time t and to the scalar field ϕ, respectively). The expansion rate in the early universe can be written as:

$$H^2 = \frac{8\pi}{3m_{Pl}^2}\left[\frac{1}{2}\dot{\phi}^2 + V(\phi)\right] \tag{2}$$

where $m_{pl} = 1.2 \cdot 10^{19} GeV$ is the Planck mass (we use natural units, i.e. $h = c = k = 1$).

The slow-roll approximation holds in most of the inflationary models. This condition is valid if (Copeland *et.al.* 1993; Hodges & Blumenthal 1990)

$$\frac{m_{pl}^2}{4\pi}\left[\frac{H''}{H}\right] = \eta(\phi) << 1 \tag{3}$$

and

$$\frac{m_{pl}^2}{4\pi}|\frac{H'}{H}|^2 = \epsilon(\phi) << 1 \tag{4}$$

The second condition, since ϵ is a direct measure of the equation of state of the scalar field matter, also implies the period of accelerated expansion (Dodelson *et.al.* 1997).

In the slow roll approximation the amplitude of scalar and tensor perturbations are related to the inflationary potential as follows (Copeland *et.al.* 1993):

$$A_S(\phi) = \sqrt{\frac{2}{\pi}}\frac{1}{m_{pl}^2}\frac{H^2}{|H'|} \tag{5}$$

and

$$A_T(\phi) = \frac{1}{\sqrt{2}\pi}\frac{H}{m_{pl}} \tag{6}$$

We can relate the wavelength, λ, and the Hubble parameter during inflation, $H(\phi)$, with the scalar field by writing:

$$\frac{d\ln\lambda}{d\phi} = \frac{\sqrt{4\pi}}{m_{pl}}\frac{A_S}{A_T} \tag{7}$$

and

$$\frac{\partial \ln H}{\partial \phi} = \frac{\sqrt{4\pi}}{m_{pl}} \frac{A_T}{A_S}, \tag{8}$$

respectively.

Let us define the spectral equations for scalar and tensor components as follows:

$$A_S^2(k) = A^2(\frac{k}{k_0})^{n_S - 1} \tag{9}$$

and

$$A_T^2(k) = B^2(\frac{k}{k_0})^{n_T} \tag{10}$$

where $k_0 = H_0$ is the wavenumber of a fluctuation which re-enters the horizon at the present time, and A and B are constants. It is easy to see that $n_T = -2\epsilon(k)$ if $\lambda = \lambda_0$, and $n_T = 0$ if $\lambda \to 0$ (Lidsey *et.al.* 1997).

We define the ratio of amplitudes of the scalar and tensor modes by:

$$r = \sqrt{\epsilon(k_0)} = \frac{B}{A} \tag{11}$$

By solving Eq.(7) and assuming $n_T \sim 0$, the scalar field can be written as a function of the wavelength:

$$\phi(\lambda) = \phi_0 + \phi_1 \left[(\frac{\lambda}{\lambda_0})^{\frac{n_S - 1}{2}} - 1 \right] \tag{12}$$

where ϕ_0 is a constant, to be found from boundary conditions, and $\phi_1 = \frac{r}{n_S - 1} \frac{m_{pl}}{\sqrt{\pi}}$.

Furthermore, Eq.s (12) and (8) allow us to find the Hubble parameter $H(\phi)$ during inflation:

$$H(\phi) = H_i \exp(\frac{r^2}{n_S - 1} \xi^2) \tag{13}$$

where $\xi = \frac{\phi + \phi_1 - \phi_0}{\phi_1}$ and H_i is a constant.

The potential can be written in terms of the Hubble parameter:

$$V(\phi) = \frac{3m_{pl}^2}{8\pi} H^2(\phi) \tag{14}$$

At this point, we can define the relation between the quadrupole multipoles of the CMB anisotropy generated by scalar and tensor perturbations: C_2^S and C_2^T, respectively. To do this we will follow the calculations done by (Souradeep & Sahni 1992) in which both C_2^S and C_2^T were found as a function of $H(\phi)$ at $\lambda = H_0^{-1}$. So we have:

$$C_2^S = \frac{2\pi^2}{25} f(n_S) \frac{1}{m_{pl}^4} \frac{H^4}{(H')^2} \tag{15}$$

$$C_2^T = \frac{2.9}{5\pi} \frac{H^2}{m_{pl}^2} \tag{16}$$

and

$$\frac{C_2^T}{C_2^S} = \frac{29}{4\pi^3} \frac{m_{pl}^2}{f(n_S)} \frac{(H')^2}{H^2} \tag{17}$$

where

$$f(n_S) = \frac{\Gamma(3-n_S)\Gamma(\frac{3+n_S}{2})}{\Gamma^2(\frac{4-n_S}{2})\Gamma(\frac{9-n_S}{2})} \tag{18}$$

Using Eq.(13) we can write:

$$\frac{\partial \ln H(\phi)}{\partial \phi} = \frac{2\sqrt{\pi}}{m_{pl}} r\xi \tag{19}$$

Therefore, at $\phi = \phi_0$ (*i.e.* $\xi = 1$), we have:

$$R(n_S) \equiv \frac{C_2^T}{C_2^S} = \frac{29r^2}{\pi^2 f(n_S)} \tag{20}$$

As we can see from the equation above, the tensor to scalar quadrupole ratio R is related to the slow-roll parameter ϵ. Eq. (20) identifies a region in the (n_S,R) space of values where the slow-roll condition is satisfied. Furthermore, as $\epsilon < 1$ only if the universe has undergone a period of accelerated expansion, one can use this equation to test the inflationary scenario.

In the same way, we can use Eq.(19) in Eq.(3) in order to find:

$$2\eta = n_s - 1 + 2r^2 \tag{21}$$

so the slow roll condition (4) implies Eq. (3) if $n_s \sim 1$.

Using Eq.(14), we can now write the potential as

$$V(\phi_0) = \frac{15}{23.2} C_2^T m_{pl}^4 \tag{22}$$

Therefore, the measurement of the contribution to the quadrupole anisotropy of tensor fluctuation, C_2^T, allows us to estimate the size of the potential responsible for inflation.

3. CMB Anisotropy

3.1. Method

We use a set of the most recent CMB anisotropy detections, both on large and degree angular scales, in order to estimate the amplitude of tensor fluctuations. The likelihood of the assumed independent CMB anisotropy data is (see de Bernardis *et.al.* 1997):

$$\begin{aligned} \mathcal{L} &= \prod_j \frac{1}{(2\pi[({\Sigma_j}^{(the)})^2 + (\Sigma_j^{(exp)})^2])^{1/2}} \\ &\times exp(-\frac{1}{2}\frac{[{\Delta_j}^{(exp)} - \Delta_j^{(the)}]^2}{(\Sigma_j^{(the)})^2 + (\Sigma_j^{(exp)})^2}) \end{aligned} \tag{23}$$

where Δ_j^{exp} and Δ_j^{the} are the experimentally detected and theoretically expected mean square anisotropy, respectively. The $(\Sigma_j^{(the)})^2$ and $(\Sigma_j^{(the)})^2$ are the respective cosmic and experimental variances. Obviously, the likelihood depends on the parameters of the cosmological model. Although a complete analysis should cover all the parameter space, here we restrict ourselves to flat models ($\Omega_0 = 1$) composed of baryons ($0.01 \lesssim \Omega_b \lesssim 0.14$), cold dark matter ($\Omega_{CDM} \gtrsim 0.7$), hot dark matter ($\Omega_\nu \lesssim 0.3$), photons and massless neutrinos. As shown in (de Bernardis *et.al.* 1997; Ma & Bertschinger 1995; Dodelson *et.al.* 1996) the angular power spectrum of MDM models differs from pure CDM by less than 10% in the angular scales of

interest. Given the poor sensitivity of the available CMB anisotropy detections at degree angular scales, we restrict ourselves to pure CDM models, keeping in mind that basically the same power spectrum is also expected for MDM models. The predictions of CDM and MDM models for the matter power spectrum obviously differ, and in a substantial way: we will discuss this point in more detail below.

Here we keep as free parameters Ω_b and h. Both parameters affect the positions and amplitudes of the so-called Doppler peaks of the angular power spectrum. In fact, changing Ω_b at fixed h changes the pressure of the baryon-photon fluid before recombination, increasing its oscillations below its Jeans length. A larger baryon to photon ratio will increase the compressions (which produce the even peaks in C_ℓ for inflationary models) and decrease the rarefaction (odd peaks for inflationary models). Lowering h at fixed Ω_b changes the epoch of matter-radiation equality: potentials inside the horizon decay in a radiation dominated era but not in a fully matter dominated one. The combination $\Omega_b h^2$, which actually appears in the calculations, is also constrained by primordial nucleosynthesis arguments (Copi *et.al.* 1995): $0.01 \lesssim \Omega_b h^2 \lesssim 0.026$. Moreover, from globular cluster ages, $0.4 \lesssim h \lesssim 0.65$ (Kolb & Turner 1991).

We will also explore variations in the spectral index of the (scalar) primordial power spectrum n_S. We restrict ourselves to values of $n_S \lesssim 1.5$, to be consistent with the absence of spectral distortions in the COBE/FIRAS data (Hu *et.al.* 1994). A parameter independent normalization for the power spectrum can be expressed in terms of the amplitude of the multipole C_{10}. We define the parameter $\mathcal{A} \equiv A/A_{COBE}$ as the amplitude $\mathcal{A}$ of the power spectrum (considered as a free parameter) in units of A_{COBE}, the amplitude needed to reproduce $C_{10} \sim 47.6 \mu K^2$, as observed on the COBE-DMR four-year maps (Bunn 1997).

Finally, for tensor fluctuations, we will assume $n_T = 0$. In fact, variations in the tensor spectral index in the range $-1 \lesssim n_T \lesssim 0$ do not give appreciable changes in the structure of the C_ℓ's, given the cosmic variance and the current experimental sensitivity. We parameterize the amplitude of these tensor fluctuations with R, defined in Eq. (22). So, in the end, we will consider only five quantities as free parameters: $\mathcal{A}$, n_S, R, Ω_b and h.

We have computed the angular power spectrum of CMB anisotropy by solving the Boltzmann equation for fluctuations in CMB brightness (Peebles & Yu 1970; Hu *et.al.* 1995). Our code is described in (de Bernardis *et.al.* 1997; Melchiorri & Vittorio 1996) and allows the study of CMB anisotropy both in cold (CDM) and mixed (MDM) dark matter models. Our C_ℓ's match to better than 0.5% for $\ell \leq 1500$ compared with those of other codes (Seljak & Zaldarriaga 1996; Ma & Bertschinger 1995). In Fig. 1 we show the C_ℓ's for different parameter choices.

The data we consider are listed in Table 1 and shown in Fig. 1. We have updated the data presented in our previous paper (de Bernardis *et.al.* 1997) to include the new results from the Tenerife, MSAM and CAT experiments. For the COBE data, we use the 8 data points from Tegmark & Hamilton 1997, that have the advantage of uncorrelated error bars.

3.2. Results

The best fit parameters (i.e. those which maximize the likelihood) are (with 95% confidence): $n_S = 1.23^{+0.17}_{-0.15}$, $R = 2.4^{+3.4}_{-2.2}$, with $\mathcal{A} = 0.92$, $\Omega_b = 0.07$ and $h = 0.46$. We can only put the following upper limits (at 68%) on these last two best fit values: $\Omega_b < 0.11$, $h < 0.58$.

A probability confidence level contour in the five dimension volume of parameters is obtained by cutting the $\mathcal{L}$ distribution with the isosurface $\mathcal{L}_P$, and by requiring that the volume inside $\mathcal{L}_P$ is a a fraction P of the total volume. The projections of the $\mathcal{L}_{68}$ and $\mathcal{L}_{95}$ surfaces on the $n_S - R$ plane are shown in Fig. 2.

As we can see from Fig. 2, the Likelihood contours are very broad and models with spectral index $n_S \sim 1$ and $R = 0$ are statistically indistinguishable from models with $n_S \sim 1.4$ and $R \sim 4$.

The quite large values of R for $n_S \gtrsim 1$ are due to a parameter degeneracy problem that present CMB anisotropy detections are not able to solve (see Fig. 1). In fact, increasing the contribution of tensor modes boosts the anisotropy on large scales ($>> 2^\circ\Omega_0^{1/2}$). As the theoretical predictions are normalized to COBE/DMR, adding tensor fluctuations while keeping all the other parameters fixed, actually suppresses the level of degree scale anisotropy. To counterbalance this effect, it is necessary to postulate "blue" primordial spectra, *i.e.* $n_s \gtrsim 1$. The shape of the confidence level region in the $n_s - R$ plane reflects this correlation. This degeneracy in the model prediction is actually broken at a higher angular resolution, $\ell \gtrsim 300$ say, where present experiments are particularly affected by cosmic variance, due to the very small region of the sky sampled (see Table 1). We have the following 95% C.L. upper limits on R: 0.3, 1.3, 2.5, 4.5, 7.8 and 12.5 for $n_s = 0.8$, 0.9, 1.0, 1.1, 1.2 and 1.3, respectively. At $n_s = 1.4$ and 1.5 we can put 95% C.L. lower limits of 1.0 and 2.8 on R. A quadratic fit to the maxima distribution gives:

$$R = 34.3 - 70.8 n_S + 36.5 n_S^2 \tag{24}$$

for $1.1 \leq n_S \leq 1.5$. With the above equation, we find that the tensor component can have an rms amplitude value of $\sim 28\mu k$ for $n_s = 1.1$ and $\sim 49\mu k$ for $n_s = 1.5$, while the scalar component remains at $\sim 100\mu k$.

It is interesting to see (Fig.1) that models with $n_S \sim 1.4$ and $R \sim 3$, which are well compatible with our analysis, seem to prefer a greater Hubble constant, $h \sim 0.6$. So, the gravitational wave contribution also seem to moderate the discrepancy between the value $h \sim 0.7$ (Freedman 1996), inferred by several different methods, and the value $h \sim 0.4$ (Lineweaver *et.al.* 1997) inferred by scalar-only CMB analysis.

We found that inside the 95% contour, the overall normalization amplitude, in units of A_{COBE} is $\mathcal{A} = 1 \pm 0.2$, *i.e.* all the models considered therein correspond well with COBE/DMR normalization.

The simple analysis carried out here does not take into account the correlation due to overlapping sky coverage (e.g., Tenerife and COBE, and/or MSAM and Saskatoon). We check the stability of our analysis with a jacknife test, i.e. removing one set of experimental data each time. We have a maximum variation of $3 - 4\%$ in our limits in the $n_S - R$ plane, except with the removal of COBE data that modifies our results by $\sim 10\%$. So, neglecting this correlation does not significantly change the results of our analysis. We also repeated the analysis including the possible $\pm 14\%$ calibration error to the five Saskatoon points (Netterfield *et.al.* 1997), and we did not find significant variations. In the limited cases where comparison is possible, our analysis produced results similar to those of Bond & Jaffe 1996, Lineweaver *et.al.* 1997 and Hancock *et.al.* 1997.

4. Comparison with LSS

As we have seen, blue models with a substantial tensor component agree well with CMB data. Tensor modes have dramatic effects on the matter power spectrum, reducing its normalization by a factor of $(1 + R)^{-1}$. Using the above fit formula, the tensor contribution to the CMB correlation function on the COBE/DMR scales can be between 54% for $n_s = 1.1$ and 91% for $n_s = 1.5$. In this section we want to test these models with large scale matter distribution. As is well known, CDM blue models predict a universe that is too inhomogeneous on scales $\leq 10h^{-1}Mpc$. Nonetheless, the excess power on these scales can be reduced by considering a mixture of cold and hot dark matter, i.e. mixed dark matter (MDM) models. The difference in the C_l behaviour between a pure CDM and an MDM ($\Omega_\nu \leq 0.3$) model is very tiny, $\leq 2\%$ up to $l \sim 300$ and $\leq 8\%$ up to $l \sim 800$ (see, for example De Gasperis *et.al.* 1995). Therefore, the

results of our CMB analysis are the same in this kind of model. In Figure 3, MDM matter power spectra from models that agree with CMB data are shown. The data points are an estimate of the linear power spectrum from Peacock & Dodds 1994, assuming a CDM flat universe and bias values between Abell, radio, optical, and IRAS catalogs $b_A : b_R : b_O : b_I = 4.5 : 1.9 : 1.3 : 1.0$ with $b_I = 1.0$. As shown in (Smith *et.al.* 1997) recovered linear power spectra of CDM and MDM models are nearly the same in the region $0.01 \leq k \leq 0.15 h Mpc^{-1}$ but diverge from this spectrum at higher k, so we restrict ourselves to this range. The χ^2 (with 11 degrees of freedom) are 15, 10, 21, 9, 37, 53 for models in Figure 3 with $(1.4, 3.3)$, $(1.3, 3.9)$, $(1.2, 1.3)$, $(1.1, 0.6)$,$(1.0, 0.1)$ and $(0.9, 0)$ in the (n_s, R) space. So, models with a large tensor contribution on COBE scales and blue spectral index seem to agree well also with the shape of matter distribution on large scale. The values for the σ_8, computed with CMBFAST (Seljak & Zaldarriaga 1995), are 0.69, 0.61, 0.66, 0.63, 0.63, 0.74, in very reasonable agreement with the value of $\sigma_8^{IRAS} = 0.69 \pm 0.05$ (Fisher *et.al.* 1994) derived from the IRAS catalog.

Whether IRAS galaxies are biased is still under debate. Analysis from cluster data (Eke *et.al.* 1996, Pen 1998, Bryan and Norman 1998), shows a preferred value of $\sigma_8 \sim 0.5 - 0.6$ with few percent error bars. Analysis from peculiar velocities (Zehavi 1998) results in a larger value $\sigma_8 = 0.85 \pm 0.2$, which seems to be in severe conflict with the cluster data. Thus, the theoretical values of σ_8 for blue MDM models with a relic gravitational wave background are between the σ_8 values derived from cluster abundance and peculiar velocities. In any case, the likelihood of the CMB data is quite flat around its maximum. So, it is easy to find models, statistically indistinguishable from the best fit models, with σ_8 nearer either to 0.5 or to 0.8.

Because of statistical and/or systematic uncertainties we do not consider it appropriate to put more than qualitative conclusions on these results, but still one can say that the lower matter normalization due to the tensor component helps the blue MDM models to match the LSS data.

5. Conclusions

Our main conclusions, are as follows:

1. The conditional Likelihood shows a maximum at $n_S = 1.23^{+0.17}_{-0.15}$, $R = 2.4^{+3.4}_{-2.2}$, with $\mathcal{A} = 0.92$, $\Omega_b = 0.07$ and $h = 0.46$. Thus, there is some evidence that a tensor component can be present, and in a substantial way, in models with n_s greater than one. Inflationary models of this type have been investigated by Copeland *et.al.* 1993 and by Lukash & Mikheeva 1996 and thus belong to the class of hybrid

inflationary models (Kinney, Dodelson & Kolb 1998). The general form of the potential can be written as $V(\phi) = V_0 + \frac{1}{2}\mu^2\phi^2$ At the end of inflation, the inflationary potential $V(\phi)$ is not equal to zero, being V_0 of the order of $\sim (610^{16} Gev)^4$. In order to be consistent with the present vacuum energy $\leq (10^{-30} Gev)^4$, one additional field is necessary to finish inflation. The inclusion of this field does not change the conclusion of our analysis, since it affects only the high frequency region of the GW spectrum ($\sim 100 MHz$). For models on the best fit curve (Eq.24), $V(\phi_0)$ belongs to the interval $4.3 \cdot 10^{-11} m_{pl}^4 < V_0 < 1.3 \cdot 10^{-10} m_{pl}^4$. In Fig.2 we plot Eq.(24) with the condition $\epsilon = 1$. The region below this curve in the $n_S - R$ plane is where the slow roll approximation is valid. As we can see, models on our best fit curve satisfy this condition, even if models with $\epsilon \geq 1$ are compatible with observations.

Approaching the limiting region $\epsilon = 1$, higher order terms in the slow roll approximation became valuable. This leads to changes in our conclusions on the potential by a factor $1 - \epsilon/3 \sim 30\%$ (Kinney, Dodelson & Kolb 1998).

2. The 95% region on the $n_S - R$ plane includes a wide range of parameters. This means that the presently available data set is not sensitive enough to produce precise determinations for n_S and R. Systematic and statistical errors in the different experiments are still significant, but, as we have shown, the difficulties involved in such determinations are mainly due to a degeneracy in these parameters. So, the (n_S, R) degeneracy has important consequences for tests of the inflationary theory: increasing the scalar spectral index and the tensor component lead to a break in the slow roll approximation, but it also produces CMB power spectra near to the scale invariant one. Therefore it is difficult from the present CMB data to see if the slow roll condition is correct.

Furthermore, current CMB results on the normalization of the matter power spectrum and/or its spectral index can be biassed and/or anti-biassed by a huge tensor contribution. As we can see from Fig.1, this degeneration also has effects on the constraints of the remaining cosmological parameters, being a model with $h \sim 0.6$ statistically indistinguishable from a model with $h \sim 0.4$.

The inflationary background of primordial gravitational waves is assumed detectable mainly through CMB experiments. The local energy density of this background is, in the most optimistic situation, extremely low, with $d\Omega_{GW}h^2/dlogk \sim 10^{-16}$ at frequencies $10^{-15} Hz < f < 10^{15} Hz$. The tenuity of this signal makes the degeneracy in the n_S and R parameters much more worrying than similar degeneracy in other parameters (e.g. h and Ω_b) that could be constrained through other measurements.

3. "Blue" MDM models with a tensor contribution, are in reasonable agreement with the present values

of σ_8, and with the shape of the matter power spectrum inferred by the Peacock & Dodds 1994 analysis. A tensor contribution could also be a viable mechanism in order to reconcile these models with a low value for the σ_8 around ~ 0.5 (Henry & Arnaud 1991).

This being the situation, a measure of the structure of the secondary peaks becomes a crucial test for the presence of tensor perturbations. Using the above best fit equation, we can make some predictions regarding future detections. We found that an experiment with a window function probing the multipoles $500 \leq \ell \leq 680$, will measure a total rms anisotropy of $28.3\mu K$ for $n_s = 1.1$, and $34.4\mu K$, with $n_S = 1.5$. An $\sim 20\%$ difference that could be proven, when the sensitivity of these experiments is within a few μk, with an improved sky coverage. Polarization measurements at intermediate angular scales can also be helpful (Sazhin 1984, Polnarev 1985, Sazhin & Benitez 1995, Sazhin 1996). The possibility of a direct separation of scalar perturbations from tensor perturbations by the method of decomposition of Stocks parameters in sets of spin ± 2 spherical harmonics seems extremely promising (Kamionkovsky & Kosowsky 1996, Seljak & Zaldarriaga 1996, Sazhin & Shulga 1996).

Possibly a definitive answer will come when future CMB experiment provides a clear and robust picture of sub-degree angular scale anisotropy and polarization.

We wish to thank Paolo de Bernardis, Ruth Durrer, Giancarlo De Gasperis, Martin Kunz and Andrew Yates. M.V.S. acknowledges the University of "Tor Vergata" for hospitality during writing part of this paper. MVS acknowledge "Cariplo Foundation" for Scientific Research and "Landau-Network - Centro Volta" for financial support during the writing the last version of this paper.

REFERENCES

Abbot L.F. and M. Wise, Nucl. Phys. **B244**, 541, 1984

Baker at al. , in press, 1997

Bennett C.L. *et.al.* ., MAP MIDEX mission proposal, 1995

Bennett C.L. *et.al.* , *Ap.J.* , **464**, L1, 1996

de Bernardis P. et al., *Ap.J.* , **422**, L33 (1994)

de Bernardis P., Balbi A., De Gasperis G., Melchiorri A., Vittorio N., *Ap.J.* , **480**, 1, 1997

Bersanelli M. *et.al.* , COBRAS/SAMBA proposal, D/SCI(96)3, 1996

Bond J.R, Efstathiou G., Tegmark M., MNRAS, **33B**, 291L, 1997

Bond J.R., Jaffe A. H., preprint, astro-ph 9610091

Bryan, Norman, *Ap.J.* , 495, 80, 1998

Bunn E., White M., *Ap.J.* , **480**, 6, 1997

E.S. Cheng, et al., *Ap.J.* , **422**, L40 (1994)

E.S. Cheng, et al., *Ap.J.* , **456**, L71 (1996)

E.S. Cheng, et al., *Ap.J.* , **488**, L59 (1997)

Copeland E.J., Kolb E.W., Liddle A.R., Lidsey J.E. Phys.Rev., **48**, p. 2529, 1993

Copi C. J., Schramm D. N., Turner M.S., Science **267**, 192, 1995

Crittenden R. *et.al.* , Phys Rev. Lett **71**, 324C, 1993

Davis M., Efstathiou G., Frenk C.S., White S.D.M., Nature **356**, 489, 1992

de Gasperis G., Muciaccia P.F., Vittorio N., *Ap.J.* , **439**, 1, 1995

Dodelson S., Knox L., Kolb E.W., Phys. Rev. Lett., **72**, P.3444, 1994

Dodelson S., Gates E., Stebbins A., *Ap.J.* , **467**, 10, 1996

Dragovan M., et al., *Ap.J.* **427**, L67, 1993

Eke et al, *M.N.R.A.S.* **263**, 282, 1996

Fisher K.B. *et.al.* , *M.N.R.A.S.* , **266**, 50, 1994

Freedman W., Proceedings for "Critical Dialogs in Cosmology", Princeton 250th anniversary, ed. N. Turok, 1996

Gundersen J.O., et al., *Ap.J.* **413**, L1, 1993

Gutierrez C. M. et al., Astrophys. J. **480**, L83, 1997

Dodelson S., W.H. Kinney, E. W. Kolb, preprint, Phys. Rev. D,**56**, 3207, 1997

Gawiser E., Silk J., Science, **1405**, 280, 1998

Hancock, S. *et.al.* , *M.N.R.A.S.* , submitted, 1997

Henry J.P., Arnaud K.A., *Ap.J.* , **372**, 410, 1991

Hodges H.M., Blumental G.R., Phys.Rev., **42**, p.3329, 1990.

Hu W.,Scott D., Sil, J., *Ap.J.* , **430**, L5, 1994

Hu W. *et.al.* , Phys. Rev. D, **73**, 2390, 1995

Kamionkovsky M., Kosowsky A., Stebbins A., Phys. Rev. Lett., **78**, 2058, 1997

Kinney, W. H., Dodelson S., Kolb E.W., To appear in the proceedings of the XXXIIIrd Rencontres de Moriond, "Fundamental Parameters in Cosmology", 17-24 January, Les Arcs, France

Kolb E. W., S. L. Vadas, Phys. Rev. D **50**, 2479, 1994

Kolb R., Turner M.S., The Early Universe, Addison Wesley, 1991

Liddle A., Phys. Rev. D **49**, 3805, 1994

Liddle A., Lith D.H, Roberts D., Viana P., *M.N.R.A.S.* **278**, 644, 1996

Lidsey J.E., Liddle A.R., Kolb E.W., Copeland E.J., Barreiro T., Abney M. Z. Reviews of Mod. Phys., **69**, p. 373, 1997.

Linde A., Phys. Rev. **D49**, 748, 1994.

Lineweaver, C.H., Barbosa, D., Blanchard, A., Bartlett J.G., A & A, **322**, 365, 1997

Lukash V.M., Mikheeva E.V., Gravitation and Cosmology, **2**, p.247, 1996.

Ma Chun-Pei , Bertschinger E., *Ap.J.* , **455**, 7, 1995

Markevich A.V., Starobinsky A.A., Astronomy Lett., f 22, p.483, 1996 (in russian).

Masi S., et al., *Ap.J.* **463**, L47, 1996

Melchiorri A. Vittorio N., Polarization of the microwave background: Theoretical framework, astro-ph 9610029, 1996

Netterfield *et.al.* , *Ap.J.* , **474**, 47, 1997

Peacock J.A., Dodds S.J., *M.N.R.A.S.* , **267**, 1020, 1994

Peebles P.J.E., Yu J.T., *Ap.J.* , **162**, 815, 1970

Pen Ue-Li, *Ap.J.* , 498, 60, 1998

Perlmutter S., Nature, **51**, 391 , 1998

Polnarev A. G., Sov. Astron., **29**, 607, 1985

Riess *et.al.* , AJ **116**, 1009R, 1998

Rubakov V.A., Sazhin M.V., Veryaskin A.V. Phys. Lett. **115B**, 189, 1982

Sazhin M.V. in: Modern theoretical and experimental problems of General Relativity and Gravitation. MGPI Publ., P.88 , 1984 (in russian);

Sazhin M., Benitez N., Astro. Lett. and Communications, **32**, p.105, 1995.

Sazhin M.V., Shulga V.V., Impact of Anisotropy and Polarization Measurements on Particle Physics, in: "Microwave background anisotropies", Les Arc, Savoie, France, 1996, p.351.

Sazhin M.V., Shulga V.V. Vestnik MGU, , p. 1996

Seljak U., Zaldarriaga M., Phys. Rev. Lett., **78**, 2054, 1997

Seljak U., Zaldarriaga M., *Ap.J.* , **455**, 7, 1995

Seljak U., Zaldarriaga M., Apj, **469**, 437S, 1996

Smith C.C., *et.al.* , *M.N.R.A.S. submitted*, astro-ph 9702099

Souradeep T., Sahni V. Modern Phys. Letters, **7**, p.3541, 1992.

Starobinsky A.A. Pisma v ZhETP. **30**, 719, 1979

Starobinsky A. Phys. Lett. **117B**, 175, 1982

Starobinsky A. Sov. Astr. Lett. **11**, 113, 1985;

Tanaka S.T. et al., *Ap.J.* , **468**, L81, 1996

Tegmark and Hamilton, astro-ph 9702019, 1997

Turner M.S. *et.al.* , Phys. Rev. D, **48**, 1993

Turner M. S., Phys. Rev. D **55**, 435, 1997

Wright E.L. *et.al.* , *Ap.J.* , **420**, 1, 1994

Zaldarriaga M.., Spergel D., Seljak U., *Ap.J.* , **488**, 1Z, 1997

Zehavi I., Proceedings of the MPA/ESO Conference "Evolution of Large Scale Structure: From Recombination to Garching, 1998

This manuscript was prepared with the AAS LaTeX macros v4.0.

Fig. 1.— Power spectra of CMB anisotropies for different combinations of inflationary and cosmological parameters. The data points are derived from the experiments listed in Table 1.

Fig. 2.— Confidence level (68 and 95%) regions for the spectral index n_S and the tensor to scalar quadrupole ratio $R = C_2^T/C_2^S$. The region below the black curve is where the slow-roll approximation is valid.

Fig. 3.— Matter power spectra for MDM models. All models are normalized to the 4-year COBE/DMR data using the method of Bunn and White 1997.

Table 1. CMB Anisotropy detections used in the Analysis. References are: (0) Tegmark and Hamilton 1997; (1) Hancock et al. 1994; (2) Gutierrez et al. 1997; (3) Gundersen et al. 1993; (4) Dragovan et al. 1993; (5) de Bernardis et al. (1994); (6) Masi et al 1996; (7) Tanaka et al. 1996; (8) Cheng et al. 1994; (9) Cheng et al. 1996; (10) Cheng et al. 1997; (11) Netterfield et al. 1996; (12) Scott et al. 1996; (13) Baker et al. 1997.

Experiment	Reference	$\Delta T^2(\mu K^2)$	$\geq 68\%(\mu K^2)$	$\leq 68\%(\mu K^2)$	Sky Coverage	ℓ_{eff}
COBE1	0	25.2	183	25.2	0.65	2.5
COBE2	0	212	126	128	0.65	3.3
COBE3	0	256	96.5	96.9	0.65	4.1
COBE4	0	105.5	48.3	48.2	0.65	5.5
COBE5	0	101.9	26.5	26.4	0.65	8.1
COBE6	0	63.4	19.11	18.9	0.65	11.6
COBE7	0	39.6	14.5	14.5	0.65	16.7
COBE8	0	42.5	12.7	12.8	0.65	25.1
Tenerife	1	1770	840	670	0.0124	20.1
Tenerife	2	3975	2855	1807	0.0124	20.1
South Pole Q	3	480	470	160	0.005	49.4
South Pole K	3	2040	2330	790	0.005	65.7
Python	4	1940	189	490	0.0006	129.0
ARGO Hercules	5	360	170	140	0.0024	118.9
ARGO Aries	6	580	150	130	0.0024	118.9
MAX HR	7	2430	1850	1020	0.0002	162.0
MAX PH	7	5960	5080	2190	0.0002	162.0
MAX GUM	7	6580	4450	2320	0.0002	162.0
MAX ID	7	4960	5690	2330	0.0002	162.0
MAX SH	7	5740	6280	2900	0.0002	162.0
MSAM93	8	4680	4200	2450	0.0007	179
MSAM94	9	4261	4091	2087	0.0007	179
MSAM94	9	1960	1352	858	0.0007	251
MSAM95	10	8698	6457	3406	0.0007	179
MSAM95	10	5177	3264	1864	0.0007	251
Saskatoon	11	1990	950	630	0.0037	99.9
Saskatoon	11	4490	1690	1360	0.0037	175.4

Table 1—Continued

Experiment	Reference	$\Delta T^2(\mu K^2)$	$\geq 68\%(\mu K^2)$	$\leq 68\%(\mu K^2)$	Sky Coverage	ℓ_{eff}
Saskatoon	11	6980	3030	2310	0.0037	283.2
Saskatoon	11	4730	3380	3190	0.0037	347.8
CAT1	12	1180	720	520	0.0001	414
CAT2	12	760	760	360	0.0001	579
CAT1	13	934	403	232	0.0001	414
CAT2	13	577	416	238	0.0001	579

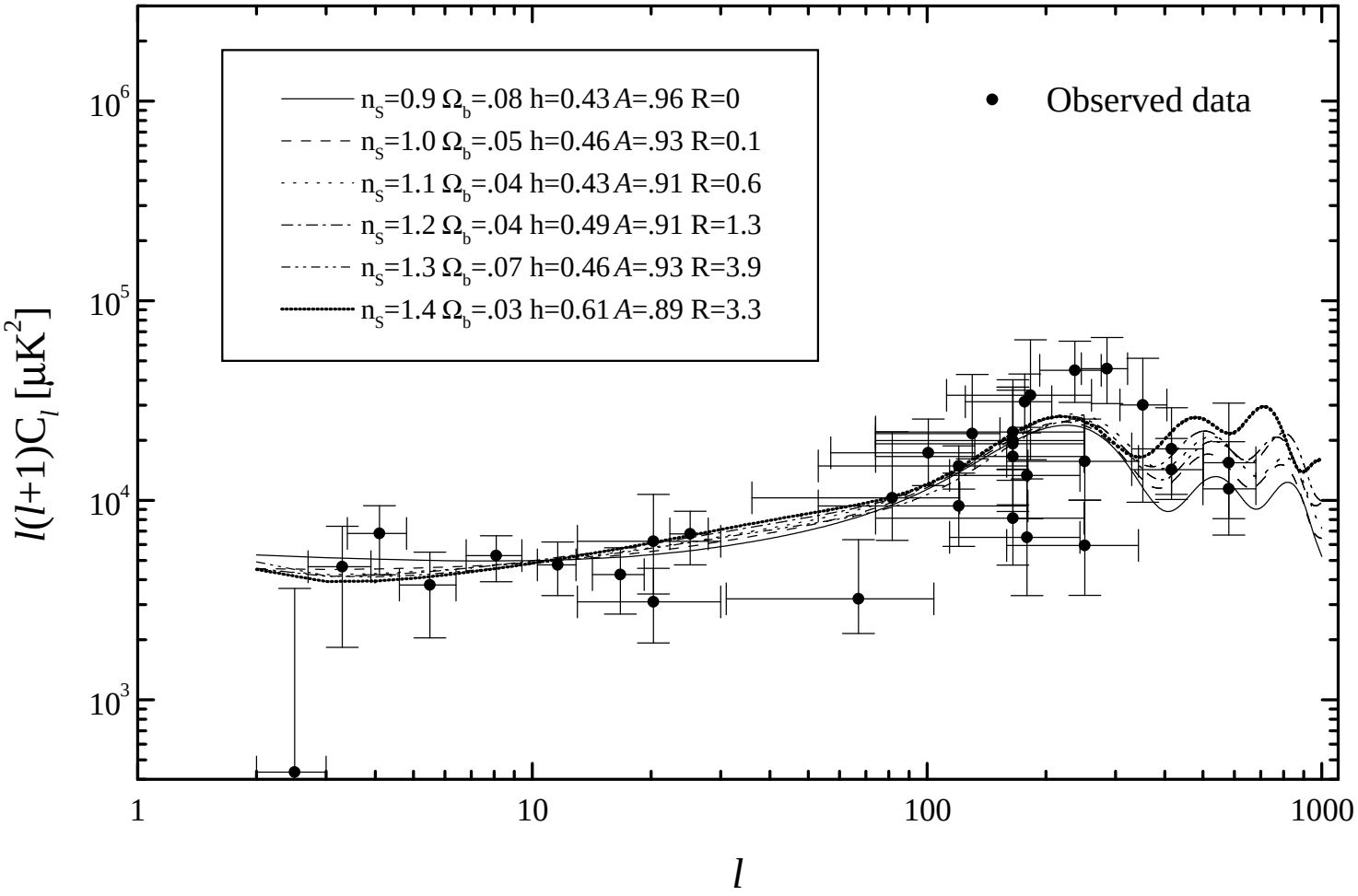
n_S=0.9 Ω_b=.08 h=0.43 A=.96 R=0
n_S=1.0 Ω_b=.05 h=0.46 A=.93 R=0.1
n_S=1.1 Ω_b=.04 h=0.43 A=.91 R=0.6
n_S=1.2 Ω_b=.04 h=0.49 A=.91 R=1.3
n_S=1.3 Ω_b=.07 h=0.46 A=.93 R=3.9
n_S=1.4 Ω_b=.03 h=0.61 A=.89 R=3.3
Observed data
$l(l+1)C_l$ [μK^2]
10^6
10^5
10^4
10^3
1
10
100
1000
l

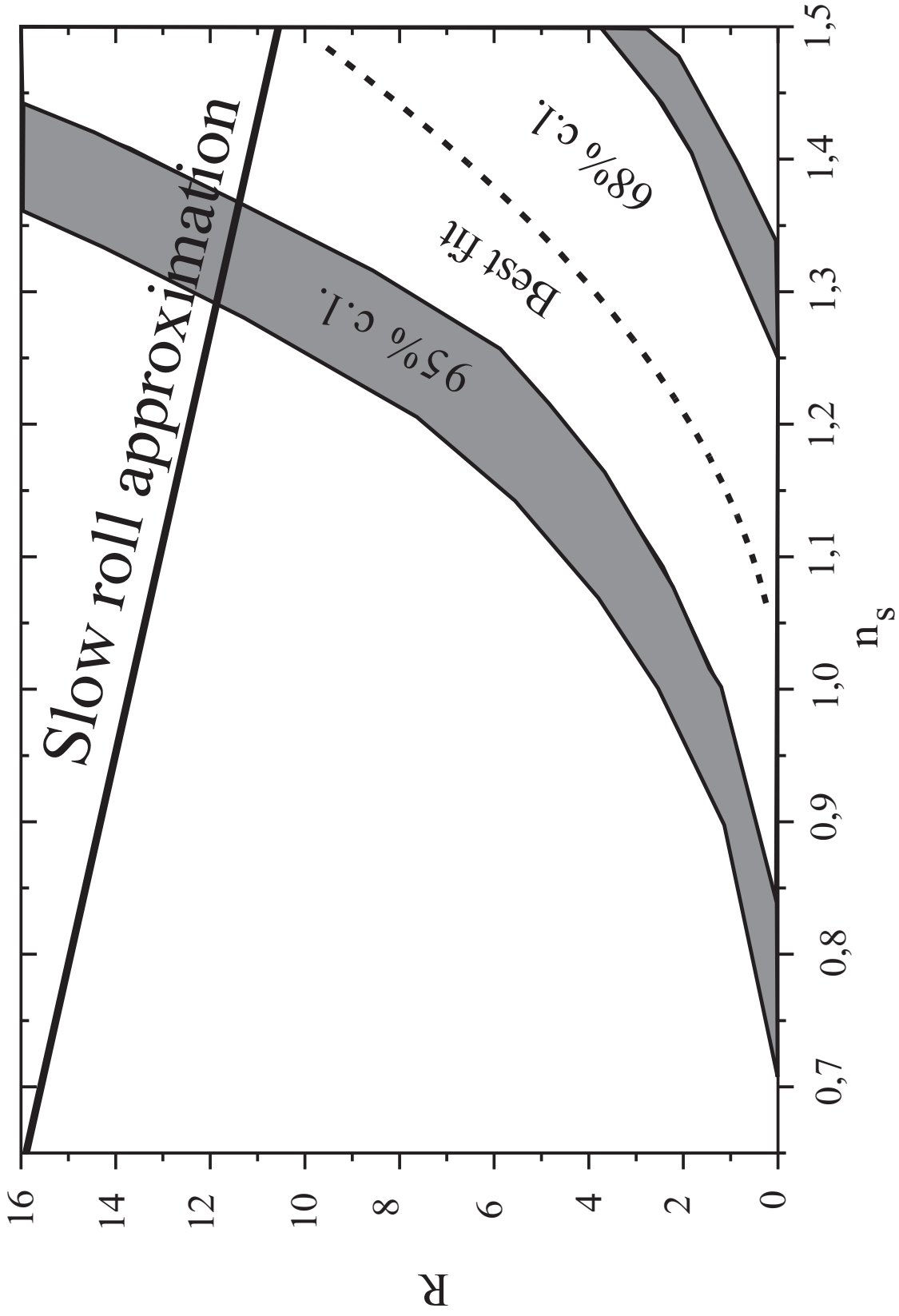
R
16
14
12
10
8
6
4
2
0
0,7
0,8
0,9
1,0
1,1
1,2
1,3
1,4
1,5
n_s
Slow roll approximation
95% c.l.
Best fit
68% c.l.

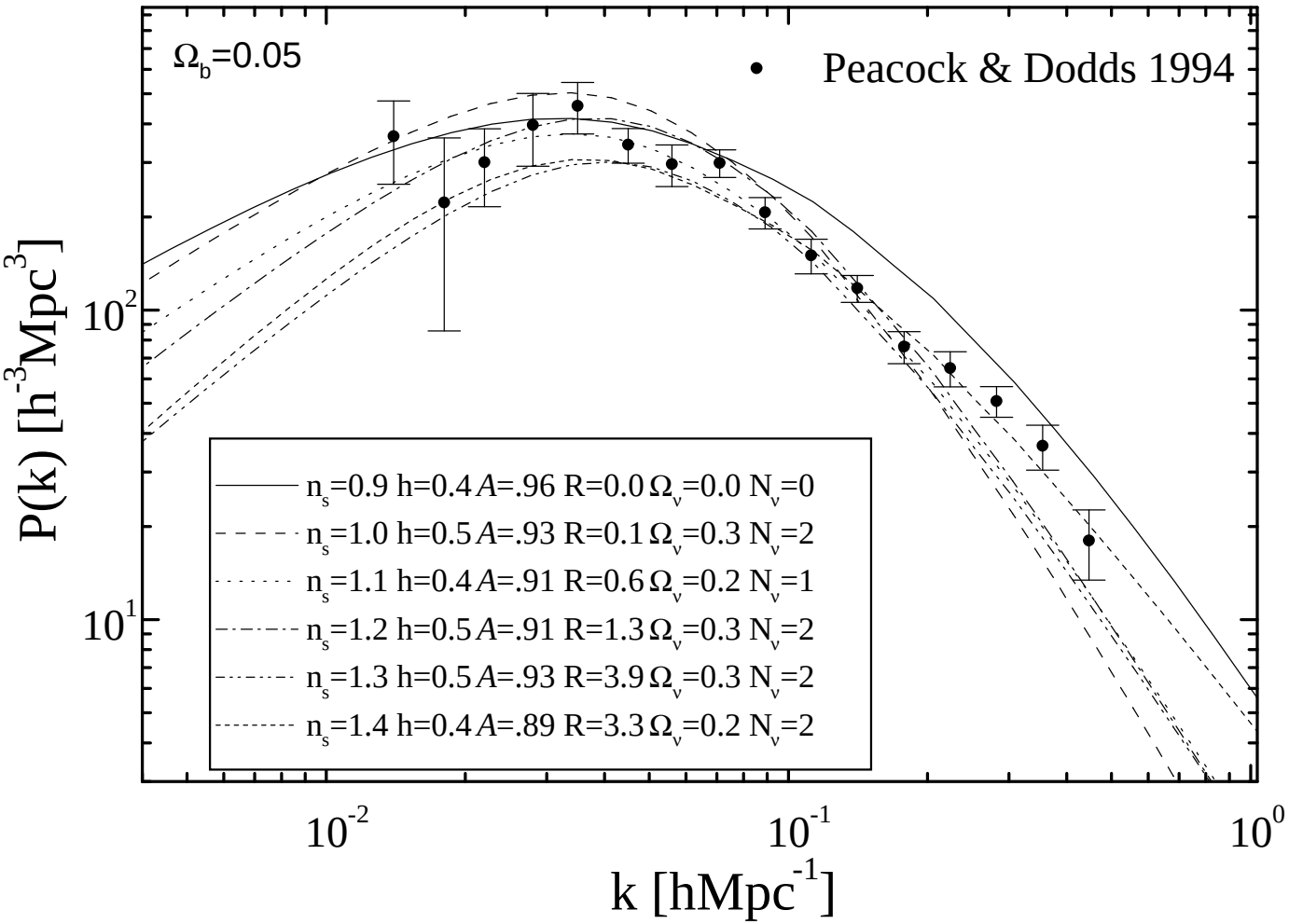
Ω_b=0.05
Peacock & Dodds 1994
n_s=0.9 h=0.4 *A*=.96 R=0.0 Ω_ν=0.0 N_ν=0
n_s=1.0 h=0.5 *A*=.93 R=0.1 Ω_ν=0.3 N_ν=2
n_s=1.1 h=0.4 *A*=.91 R=0.6 Ω_ν=0.2 N_ν=1
n_s=1.2 h=0.5 *A*=.91 R=1.3 Ω_ν=0.3 N_ν=2
n_s=1.3 h=0.5 *A*=.93 R=3.9 Ω_ν=0.3 N_ν=2
n_s=1.4 h=0.4 *A*=.89 R=3.3 Ω_ν=0.2 N_ν=2
P(k) [h^{-3}Mpc^3]
10^2
10^1
10^{-2}
10^{-1}
10^0
k [hMpc^{-1}]